Int J Infrared Milli Waves (2007) 28:315–328
DOI 10.1007/s10762-007-9215-y

Design of a CW 1 THz Gyrotron (Gyrotron Fu Cw III) Using a 20 T Superconducting Magnet

La Agusu · T. Idehara · H. Mori · T. Saito · I. Ogawa · S. Mitsudo

Received: 25 February 2007 / Accepted: 9 March 2007 / Published online: 28 March 2007

Abstract Design of a CW 1 THz gyrotron at second harmonic operation using a 20 T superconducting magnet has been described. The mode competition analysis is employed to investigate operation conditions of second harmonic mode, which is being excited at the frequency ranging from 920 GHz to 1014 GHz. The output power up to 250 watt corresponding to the efficiency of 4.16 percent could be achieved by using an electron beam with accelerating voltage 30 kV and current 200 mA. The important advantage of this gyrotron is that the single mode excitation at second harmonic, and extremely high frequency of the radiation, could be maintained even at high currents. It opens possibility to realize a high power radiation source at 1 THz. Such gyrotron is under construction at FIR Center, University of Fukui.

Keywords Gyrotron · Terahertz · Submillimeter wave · CW operation · Second harmonic · Mode competition

1 Introduction

A gyrotron is an important source of short wavelength coherent radiation. Gyrotron development is being advanced in two ways. The major way is development of high power, millimeter wave gyrotrons for heating and current drive for fusion plasma. It is being pursued worldwide and has achieved around 1MW output power for long pulse operation (longer than several tens second or quasi CW) at the frequency of 170 GHz or 140 GHz [1–4]. On the other hand, medium power, high frequency gyrotrons are being developed in several institutions in the world [5–7]. In the devices belonging to the latter class, high magnetic field and higher harmonic operations are used for increasing the operation frequency. Such gyrotrons have already covered wide frequency range in millimeter to submillimeter wavelength region and have been applied as submillimeter wave radiation sources in many fields including plasma diagnostics [8], electron spin resonance (ESR) spectroscopy [9, 10], nuclear magnetic resonance (NMR) spectroscopy [11], new medical technology [12], and so on.

L. Agusu (✉) · T. Idehara · H. Mori · T. Saito · I. Ogawa · S. Mitsudo
Research Center for Development of Far-Infrared Region, University of Fukui,
3-9-1 Bunkyo, Fukui-shi 910–8507, Japan
e-mail: laagusu@fir.fukui-u.ac.jp

Recently, terahertz sources corresponding to frequencies between 300 GHz and 3 THz have attracted considerably attention for use in both fundamental research and technologies, e.g. material sciences and engineering, solid-state physics, molecular analysis, atmospheric research, biosciences, medical treatment, food inspection, and airport security. Several different devices have been developed, investigated and successfully applied as sources of terahertz waves during the last years. The gyrotrons however have a promising advantage over the conventional vacuum electron devices as well as solid state devices for this frequency range.

The gyrotron oscillators and amplifiers rely on a resonance between the modes of an interaction structure (such as transverse electric modes of a cylindrical cavity) and the helical electron beam in a strong magnetic field. The resonator is usually overmoded since its physical dimensions are much larger than the operating wavelength. This permits high peak and average power operation even at high frequencies without risk of damage to the interaction structure. In the case of the conventional vacuum electronic devices such as the klystron and traveling wave tube (TWT) for example; the physical dimensions of their interaction structures are of the order of the wavelength. This introduces serious limitations to the output power at high frequency and makes them not feasible at frequency above 140 GHz. Solid state devices operating in the THz region have made remarkable progress recently but their output power is several order of magnitude lower compared to gyrotrons. Therefore the gyrotrons are practically the only sources of powerful radiation (several hundreds watts to several tens kilowatts) in the THz region of the electromagnetic spectrum.

The frequency of the gyrotron close to the cyclotron frequency (which is proportional to the applied magnetic field) or its harmonics. Operating the gyrotron at harmonics reduces the necessary magnetic field n times, where n=1,2,3,... is the corresponding harmonic number. For example, in order to achieve 1 THz radiation, a gyrotron operating at second harmonic (n=2) requires magnetic field with maximum intensity of only 19 T corresponding to 502 GHz fundamental (n=1) frequency if one uses electron beam with accelerating voltage 30 kV. It is well-known however that the harmonic interaction is inherently less efficient compared to the fundamental operation. Additionally, it is prone to more serious problems with mode competition. Therefore, more careful design of the tube is needed in order to ensure selection and excitation of desired mode and to avoid competing (usually fundamental) modes.

Our gyrotrons developed in FIR FU named Gyrotron FU Series belong to the second type of gyrotrons, that is, medium power high frequency gyrotrons. This series has demonstrated the following achievements: 1) frequency step-tunability in wide range in millimeter to submillimeter wavelength region (from 38 to 889 GHz); 2) the highest frequency (889 GHz) corresponding to the wavelength of 377μm by using second harmonic operation at the field intensity of around 17 T; 3) modulation of amplitude and frequency of the output radiation; 4) stabilization of amplitude and frequency; 5) high harmonic operations up to fifth (in a Large Orbit Gyrotron); and 6) high-purity mode operations at many cavity modes by installation of a carefully designed cavity [13]. Also, we have achieved mode conversion from circular waveguide modes to a Gaussian mode for applications of our gyrotrons to many fields [14]. Recently, the breakthrough of 1 THz in pulse operation was achieved in our Research Center [15].

For many applications however CW radiation sources are needed. In order to meet this requirement and to expand the application of our devices to new fields of research and technology we have started the development of novel series, namely Gyrotron FU CW Series.

The first member of this new line of tubes is Gyrotron FU CW I. It operates in CW at 300 GHz and delivers output power of 1.8 kW [16]. The next one, the Gyrotron FU CW II, is being developed as a source of CW radiation with frequency 395 GHz and output power 100 W [17]. These gyrotrons will be used for development of high power THz technologies, plasma diagnostics, NMR spectroscopy with DNP enhancement of the signal, *etc.*

In this paper, we report the design of a CW gyrotron with an output power 100 watt at frequency of 1 THz. Since this prospective device will be the third member of the novel series developed at FIR FU Research Center it will be referred to as Gyrotron FU CW III. This tube will utilize a newly obtained 20 T superconducting magnet (designed and constructed by JASTEC Co.) and will be operated at second harmonic of the cyclotron frequency. The initial test of the magnet has been successfully carried out. In this paper we present our design consideration for development of novel gyrotron using this magnet.

2 Gyrotron design considerations

The goal of this design is to construct a new gyrotron which is capable to generate radiation with CW power of several hundreds watts and frequency 1 THz at the second harmonic. The novel design of the 1 THz CW gyrotron oscillator is based on a previous pulse 1 THz

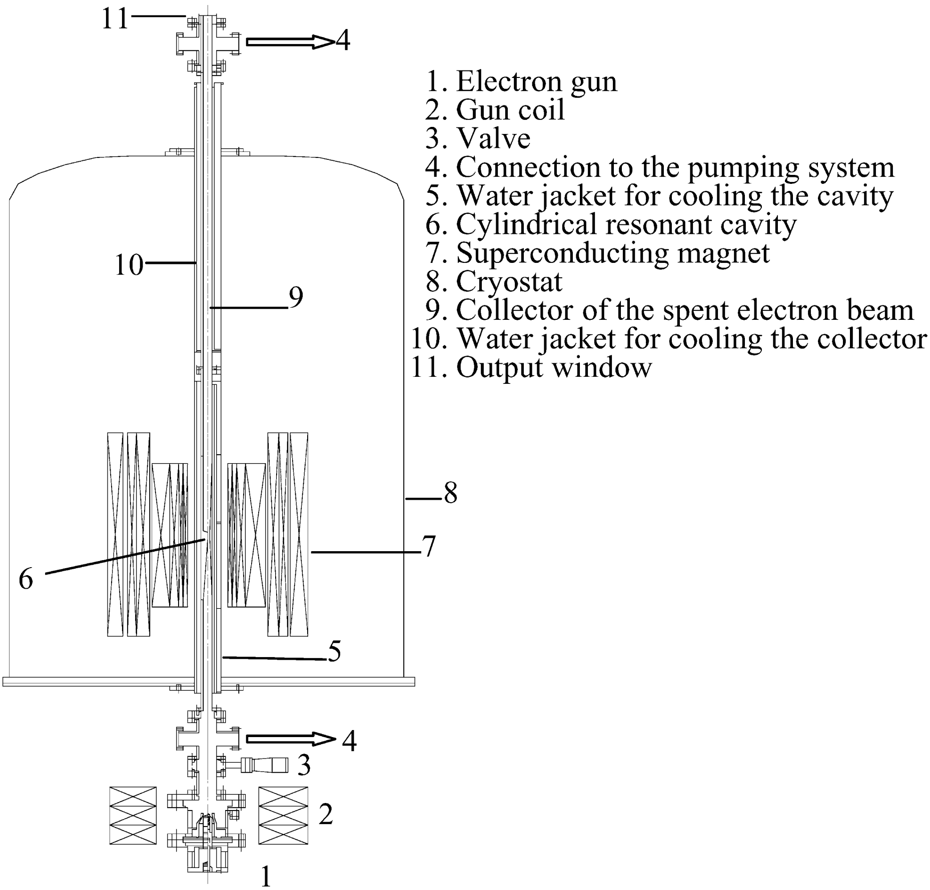

Fig. 1 The cross-sectional view of the cylindrically symmetric 1 THz CW gyrotron tube. The gyrotron tube is approximately 2.5 m long and magnet bore diameter is 5 cm.

gyrotron oscillator built at FIR Center, University of Fukui [15]. The experimental tests using a 21 T pulse magnetic system have been carried out with the radiation frequency ranging from 395 GHz to 1.014 THz. Operational characteristics of this design include the ability to excite a second harmonic cavity mode without competition with the fundamental modes, at a high power level in THz regime.

A cross-sectional view of the CW 1 THz gyrotron system is shown in Fig. 1. The axes of the gyrotron tube and electron beam are aligned with the axis the 20 T superconducting magnet. There are two pumping bores. The first one is located near the electron gun to assure the vacuum condition inside the tube. The second one is placed after the collector in order to keep the vacuum despite the out-gasing from the electron collector as well as the resonator. In the continuous-wave (CW) operation, the temperature of the cavity increases during the operation. It has been observed in the experiment that there was an influence of increasing cavity temperature on the shift of the frequency and output power of CW gyrotron [18, 19]. This observation suggests that a cooling system surrounding the cavity is absolutely necessary. The water jacket with a constant flow rate is installed surrounding the whole gyrotron tube, including the collector, to maintain the tube temperature at a permissible level for stable operation of the gyrotron. The main function of the collector is to dissipate the energy of the spent electron beam but it also serves as a microwave waveguide, which transmits the radiation generated in the cavity to the output window. To allow pumping at the collector end, several small holes (with diameter less than the wavelength) are made there. The total length of tube including the collector is 2.5 m. Sets of two stages for horizontal adjustment are located at both the top and the bottom part of the cryostat and are used to align the gyrotron tube with respect to the magnetic field of the superconducting magnet, thereby aligning the axis of the electron beam. The gyrotron tube is demountable which enables to change some parts of it.

2.1 Superconducting magnet

The superconducting magnet with 5 cm of inner bore has eight parts of cylindrically symmetric coils with total number of windings that amount to 30676. There are four Nb_3Sn coils and NbTi coils. The expected maximum field intensity is 20 T at the current of 290 A. Magnetic field inhomogeneity 2 cm away from the center of magnet is only 0.11 percent. The distance between the emitter of electron gun and the center of superconducting coil is approximately 82 cm. The superconducting magnet provides maximum field intensity of 0.21 T at the cathode.

2.2 Electron gun

The electron gun is a triode magnetron injection gun (MIG) type with a configuration, which has been used for several gyrotrons in our center, Gyrotron FU V [20], 1 THz pulse gyrotron [15], and Gyrotron FU CW II (395 GHz) [17]. Its geometry is shown on Fig. 2. The electron optical performance of the gun for the new operational conditions have been investigated by means of EPSOR code [21], which is based on an adequate and fully relativistic self-consistent physical model which takes into account initial velocities and space charge effects.

Three water-cooled additional coils installed in the gun region are important part of the electron optical system (EOS). They are used in order to tailor the necessary magnetic field for the initial beam formation in the cathode-anode region as well as for fine tuning of the beam parameters. The maximum field intensity provided by the gun coil is 0.13 T at the

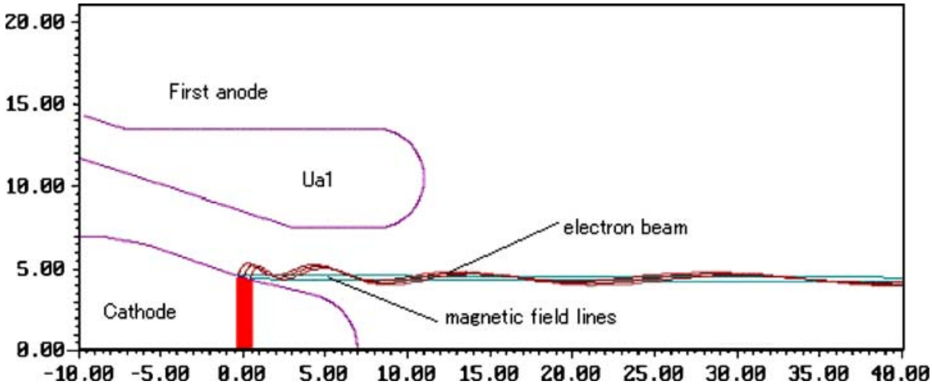

Fig. 2 Configuration of the gun and electron trajectories.

current of 300 A. The beam radius for excitation of desired operating modes at the second harmonic is 0.35 mm and as the simulation shows can be obtained at magnetic field 0.11 T at the emitter. The superconducting magnet itself produces 0.21 T at the cathode. Therefore in order to obtain the necessary magnetic field at the emitter and control precisely its value the additional gun coils are excited in such a way as to produce field with opposite direction compared with the main coils of the superconducting magnet. By varying the current through gun coils one can adjust the beam radius from 0.28 mm to 0.58 mm.

Illustrative results from trajectory analysis of the EOS are shown on Fig. 2. As a whole the data obtained in numerical experiments suggest that this configuration is capable to produce relatively high quality helical electron beam with nominal pitch factor around 1.1 and velocity spread less than 10 percent.

2.3 Interaction cavity

The resonant interaction structure of the gyrotron consists of a cylindrical cavity with length 10 mm and radius 1.95 mm and two linearly tapered sections. The down-taper and the up-tapers have slopes 5.5° and 22.3° respectively (see in Fig. 3). Figure 3 shows also the axial profile of the amplitude of the selected cavity mode, $TE_{4,12}$. The material of the gyrotron

Fig. 3 The cross-section of a 1 THz GHz gyrotron cavity with the axial field profile for the cavity mode $TE_{4,12}$ at second harmonic. Input taper: L_1=5 mm, θ_1=5.1°; Middle section R= 1.95 mm, L=10 mm; output taper: L_2=5 mm, θ_2=22.3°.

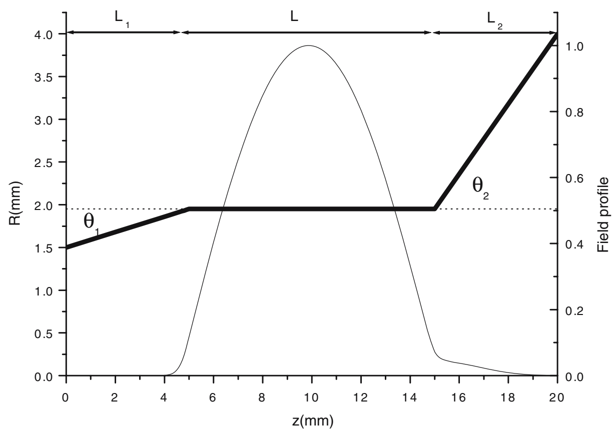

Table 1 Parameters of the electron beam.

Vc (kV)	I_b(A)	R_b(mm)	α
30	0.2	0.35	1.1

cavity is copper. Based on the cold-cavity calculation, the frequency and total Q-factor are estimated as being approximately 1013.67 GHz and 23720, respectively.

3 Mode competition

Mode competition study is needed in order to find a set of appropriate operational parameters that correspond to excitation of desired mode at second harmonic of the cyclotron frequency and avoid competition with the fundamentals and other second harmonic modes. Mode competition can be studied by the self-consistent, multimode, time-dependent system of equations [22] for the dimensionless (normalized) transverse momentum p of an electron and the amplitude f_s of the RF field of mode with index s:

$$\frac{\partial p}{\partial \varsigma} + i\left(|p|^2 - 1\right)p = i\sum_s (p^*)^{n_s-1} f_s \exp\left[i(\Delta_s\varsigma + \psi_s)\right], \tag{1}$$

$$\frac{\partial^2 f_s}{\partial \varsigma^2} - in_s\frac{\partial f_s}{\partial \tau} + n_s\delta_s = I_s\frac{1}{4\pi^2}\int_0^{2\pi}\int_0^{2\pi} p^{n_s} d\theta_0 \exp\left[-i(\Delta_s\varsigma + \psi_s)\right]d\varphi,$$

where ζ and $\tau = \frac{1}{8}\beta_\perp^4\beta_\parallel^{-2}\omega_c t$ are the normalized axial and temporal coordinates, respectively; φ is the azimuthal coordinates, $\Delta_s = \frac{2}{\beta_\perp^2}\left(\frac{\overline{\omega}_s - n_s\omega_c}{\omega_c}\right)$ is the normalized frequency mismatch between the frequency of gyrotron oscillations $\overline{\omega_s}$ and n_s-th harmonic $n_s\omega_c$ of the cyclotron frequency ω_c. Here $\psi_s = 8\beta_\parallel^2\beta_\perp^{-4}(\overline{\omega}_s - \omega_c)\omega_c^{-1}\tau + (n_s \mp m_s)\varphi$ is the phase of the mode and m_s is the azimuthal index. The parameter $\delta_s = 8\beta_\parallel^2\beta_\perp^{-4}\left(\overline{\omega}_s - \omega_{cut,s}(\zeta)\right)\omega_c^{-1}$ describes the variation of the cut-off frequency $\omega_{cut,s}(\zeta)$ along the resonator axis. The dimensionless current I_s includes the RF field and electron beam coupling. In the above expressions $\beta_\parallel, \beta_\perp$ have the usual meaning of the axial and transverse velocities of the electron normalized to the speed of light.

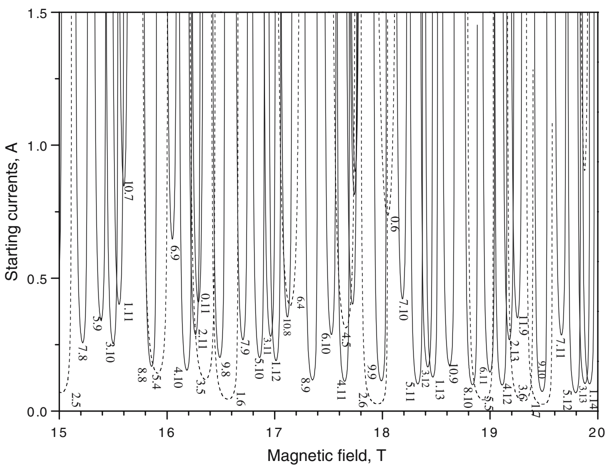

Fig. 4 Starting current of the cavity modes. Here, Vc=30 kV, R_b=0.4 mm, and α=1.1.

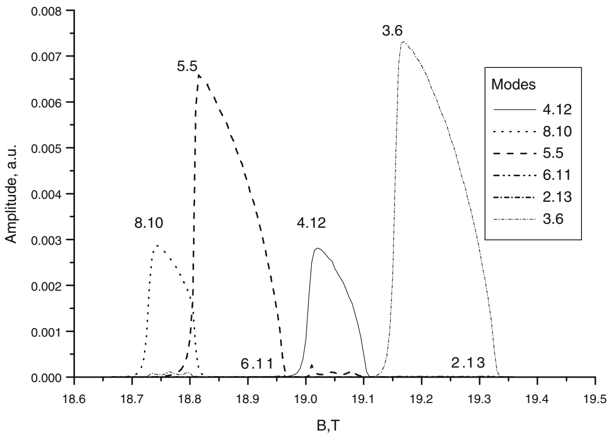

Fig. 5 Amplitudes of cavity modes at the final stage of mode competition simulation (t=75 ns) as functions of magnetic field. There are six cavity modes are included in calculation. Here, the beam parameters are taken from Table 1.

The first equation in the system (1) has to be supplemented by the initial condition $p(0) = \exp(i\theta_0), \quad 0 \leq \theta_0 < 2\pi$ and the second equation by $f(\zeta,0)=f_0(\zeta)$, where $f_0(\varsigma)$ is RF field profile obtained in the cold-cavity approximation. The boundary condition for the second equation of the system (1) can be written as usual

$$f_s(\varsigma_{out},\tau) = \frac{i}{k_s}\frac{\partial f_s(\varsigma,\tau)}{\partial \varsigma}\bigg|_{\varsigma=\varsigma_{out}}, \tag{2}$$

where $k_s = 2c\beta_{\|}\beta_{\perp}^{-2}\omega_c^{-1}\left[\overline{\omega}_s^2/c^2 - \chi_s^2(\varsigma)/R_{cav}^2(\varsigma)\right]^{1/2}$ is the dimensionless longitudinal wave number, χ_s is the eigenvalue of the mode, and R_{cav} is the cavity radius.

The electron efficiency of gyrotron can be written as

$$\eta = \frac{\alpha^2}{1+\alpha^2}\eta_{\perp}, \tag{3}$$

where $\eta_{\perp}$ is the perpendicular efficiency given by the relation:

$$\eta_{\perp} = 1 - \frac{1}{2\pi}\int_0^{2\pi}|p(\zeta_{out})|^2 d\theta_0, \tag{4}$$

and $\alpha = \beta_{\perp}/\beta_{\|}$ is the velocity ratio (pitch factor) of the electron.

Table 2 List of modes considered in the simulations at magnetic fields from 18.65 to 19.4 T.

TEmn Mode		Frequency (GHz)	Q	Harmonic number	Rotation
m	n				
4	12	1013.67	23720	2	+
8	10	999.15	22859	2	–
6	11	1007.68	23278	2	+
2	13	1017.23	23931	2	+
3	6	513.35	10668	1	+
5	5	503.64	10163	1	–

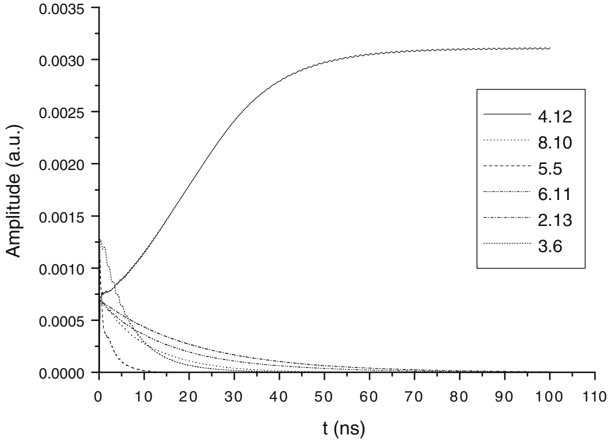

Fig. 6 Time evolution of the amplitudes of different modes at B=19.05 T.

4 Simulation results

4.1 Starting current

Figure 4 shows the starting current of each cavity mode as a function of the magnetic field intensity ranging from 14.5 T to 20 T. The electron beam parameters used in the calculation are the following: beam voltage is 30 kV, beam radius is 0.4 mm, and pitch factor is 1.1. This chart was used for an initial preliminary analysis of the mode spectrum to be performed in order to identify the potential candidates for second harmonic operation at different frequencies. It can be seen in Fig. 4 that the starting current of $TE_{4,12}$ mode at second harmonic do not overlap with the fundamentals. Some other modes such as $TE_{5,11}$ and $TE_{8,9}$ tend to be excited without competition with the fundamental by provided that the beam current, the beam radius, and the magnetic field intensity are adjusted accordingly. This very rough analysis was supplemented by more detailed mode competition calculation presented in the next section.

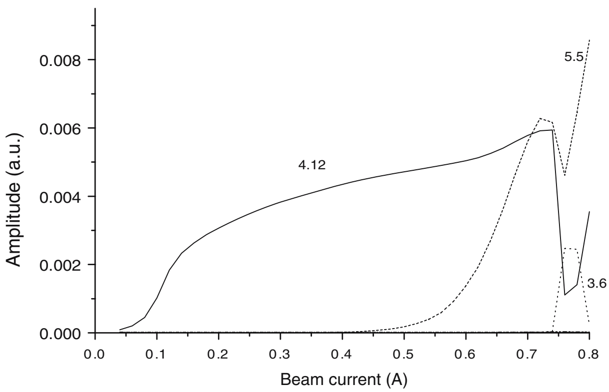

Fig. 7 The amplitude of several modes at the final stage of simulation (t=75 ms) as a function of the beam current when at B= 19.05 T. Other beam parameters as in Table 1.

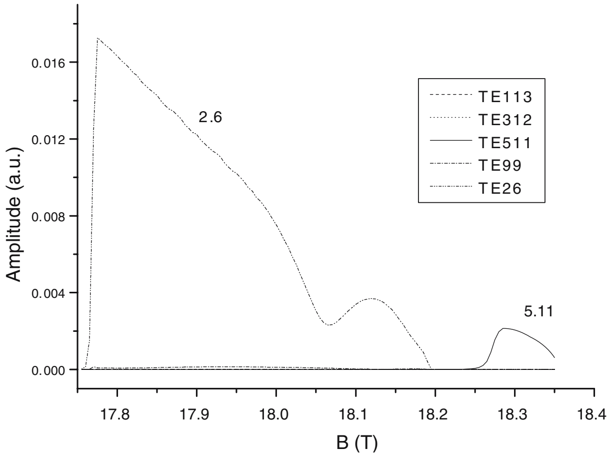

Fig. 8 Amplitude of several modes at the final stage of the simulation in mode competition scenario (t=75 ns) for different magnetic fields. The regime of single mode excitation of $TE_{5,11}$ at second harmonic is specified.

4.2 Mode competition simulations

The operation conditions of the cavity modes at second harmonic were investigated through the numerical experiments performed using a time-dependent computer code in which the model described in Sect. 3 is implemented. It allows mode interaction between up to seven cavity modes at different harmonic to be simulated simultaneously. Calculation are performed for a range of field intensity, with 0.01 T step in order to determine the operational conditions for excitation of desired cavity mode at the THz regime. At each step, equation (1) is solved for 75 ns of interaction time with 0.1 ns time step. The initial input values for the frequency, initial field profile, and Q-factor are taken from cold-cavity calculation. Normalized initial amplitude of all modes is 0.01. The final amplitude of each mode is stored together with the corresponding field intensity in the data base of numerical experiments. The electron efficiency and output power can is then calculated using of Eq. (3).

Figure 5 shows calculation result for magnetic field intensity ranging from 18.65 T to 19.4 T. The beam parameters used in calculation are cathode voltage 30 kV, beam radius 0.35 mm, and pitch factor of 1.1 (see Table 1). There are six cavity modes that could (potentially) be excited (see Table 2), namely the second harmonic modes $TE_{4,12}$ (f= 1013.67 GHz), $TE_{8,10}$ (f=999.15 GHz), $TE_{6,11}$ (f=1007.68 GHz), and $TE_{2,13}$ (f= 1017.23 GHz); and the fundamental $TE_{5,5}$ (f=503.64 GHz) and $TE_{3,6}$ (f=513.35 GHz). Among them, only 4 cavity modes: $TE_{8,10}$, $TE_{5,5}$, $TE_{4,12}$, and $TE_{3,6}$ are excited at different magnetic fields. It is seen in Fig. 5 that the desired second harmonic cavity modes $TE_{4,12}$ at

Table 3 List of cavity modes used in the simulations.

TE_{mn} Mode		Frequency (GHz)	Q	Harmonic number	Rotation
m	n				
1	13	979.66	23165	2	+
3	12	977.20	23018	2	−
5	11	972.25	22724	2	+
9	9	954.42	21659	2	−
2	6	477.65	9617	1	+

Magnetic field intensity varies from 17.75 to 18.35 T

Table 4 List of cavity modes in mode competition simulation performed to find the operating conditions for TE $_{8,9}$ mode.

TE_{mn} Mode		Frequency (GHz)	Q	Harmonic number	Rotation
m	n				
8	9	920.61	21087	2	−
1	12	902.75	21443	2	−
10	8	908.33	20350	2	−
6	10	929.90	21644	2	−
4	11	936.40	22032	2	−
4	5	469.90	9220	1	−
6	4	456.24	8547	1	+

1013.67 GHz and $TE_{8,10}$ at 999.15 GHz are excited without competition with the fundamentals. The field intensity for single mode operation of $TE_{4,12}$ is in the interval between 19.0 and 19.1 T. It has been confirmed experimentally by using a THz gyrotron with a pulse magnet [15]. In addition, $TE_{8,10}$ at second harmonic could be excited at field intensity ranging from 18.7 T to 18.8 T.

Figure 6 shows the time evolution of the amplitudes of different modes at B=19.05 T. The total electronic power and efficiency are 0.77 kW and 12.8 percent. It is seen that only $TE_{4,12}$ mode develops while the rest are suppressed.

Results of mode competition at B=19.05 T and increasing beam current are shown in Fig. 7. The amplitude of the modes at the final stage (t=75 ns) are plotted as a function of the beam current in order to specify the regime for single mode excitation of the $TE_{4,12}$ mode at second harmonic. One can see that a single mode excitation of $TE_{4,12}$ at second harmonic with a significant power takes place for the beam currents ranging from 0.1 A to 0.5 A. Then for beam currents $0.5<I_b<0.7$ A $TE_{5,5}$ at fundamental and $TE_{4,12}$ coexist. Finally, at greater currents ($I_b>0.7$ A) multi-mode interaction between of $TE_{5,5}$ and $TE_{3,6}$ at fundamental, and $TE_{4,12}$ at second harmonic takes place. The important advantage of the selected operating mode is that the single mode excitation at second harmonic and extremely high frequency of the generated radiation could be maintained at high electron beam currents. This opens possibility to achieve a high power radiation at 1 THz.

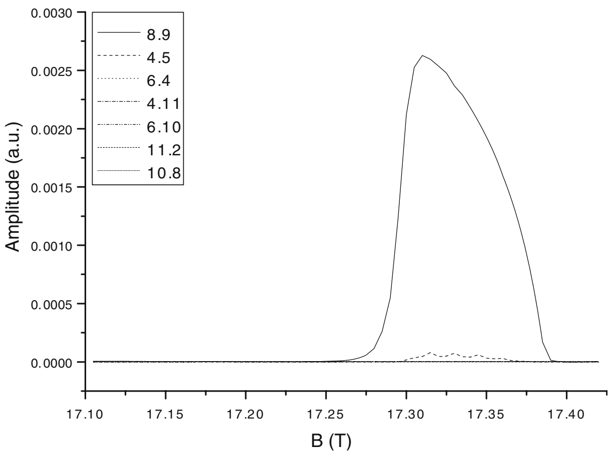

Fig. 9 Amplitudes of the modes at the final stage of the simulation in mode competition scenario (t= 75 ns) as functions of magnetic field. $TE_{8,9}$ mode at second harmonic dominates in the region between 17.27 and 17.4 T. Operating modes taken into account in the mode interactions are listed in Table 4. The corresponding beam parameters are given in Table 1.

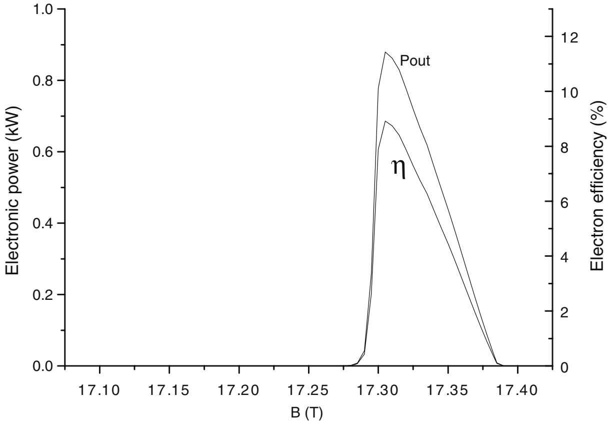

Fig. 10 The electronic power and efficiency vs magnetic field corresponding to the results in Fig. 10.

Operation condition of the cavity mode at 17.75 T<B<18.35 T is illustrated in Fig. 8. Parameters used in this calculation are listed in Table 1. Four cavity modes at second harmonic and one cavity mode at fundamental are included in the mode competition simulation (see in Table 3). The most dangerous mode is the fundamental, $TE_{2,6}$ at 477.65 GHz. As a result, $TE_{2,6}$ covers a wide regime of field intensity from 17.75 T to 18.2 T and then it is followed by excitation of $TE_{5,11}$ at 972.25 GHz ranging from 18.25 T to 18.35 T of field intensity. The $TE_{5,11}$ mode at second harmonic is the second candidate for THz radiation. The radiated output power is 0.26 kW with corresponding efficiency of 4.3 percent.

Figure 9 shows the mode competition result for field intensity ranging from 17.1 T to 17.4 T, where the second harmonic mode $TE_{8,9}$ is operated at 920.61 GHz without any disturbance from the fundamentals. Here, the beam parameters are the same as in the previous calculations (see in Table 1). The radiated power when $B=17.3$ T is 0.68 kW corresponding to an efficiency of 11.4 percent (see in Fig. 10).

4.3 Ohmic losses

The Ohmic losses in cavity are always a big concern for the high output power gyrotrons. Table 5 shows calculated Q factors and Ohmic losses as well as the total output power and efficiency. Listed four modes are excited without competition with the fundamental. One can see in Table 5 that the Ohmic losses are decreasing significantly the output power of gyrotron.

Table 5 Output power calculation by taking into account the Ohmic losses.

	$TE_{4,12}$	$TE_{8,10}$	$TE_{5,11}$	$TE_{8,9}$
Frequency, GHz	1013.67	999.15	972.25	920.61
Qdiff	72208	69590	67075	60242
Qohm	35324	34041	34367	32443
Q	23720	22859	22724	21087
Electronic power, kW (Pout+Pohm)	0.77	0.75	0.26	0.68
Electronic efficiency, %	12.8	12.5	4.3	11.4
Ohmic losses: 1_Q/Qdiff, %	67.15	67.15	66.12	64.99
Total output power, kW	0.25	0.25	0.09	0.24
Total efficiency, %	4.16	4.16	1.5	4.0

Table 6 Summary of the gyrotron parameters.

	$TE_{4,12}$	$TE_{8,10}$	$TE_{5,11}$	$TE_{8,9}$
Frequency, GHz	1013.67	999.15	972.25	920.61
Magnetic field, T	19.05	18.78	18.3	17.35
Cavity radius, mm	1.95	1.95	1.95	1.95
Cavity length, mm	10	10	10	10
Cathode voltage, kV	30	30	30	30
Beam current, mA	200	200	200	200
Beam radius, mm	0.35	0.35	0.35	0.35
Pitch factor	1.1	1.1	1.1	1.1
Q_{diff}	72208	69590	67075	60242
Q_{ohm}	35324	34041	34367	32443
Total Q_factor	23720	22859	22724	21087
Electronic power, kW (Pout+Pohm)	0.77	0.75	0.26	0.68
Electronic efficiency, %	12.8	12.5	4.3	11.4
Ohmic losses, % 1-Q/Q_{diff}	67.15	67.15	66.12	64.99
Total output power, kW	0.25	0.25	0.09	0.24
Total efficiency, %	4.16	4.16	1.5	4.0
Cathode radius, mm	4.5	4.5	4.5	4.5

5 Gyrotron parameters

Based on these preliminary simulation results the first design of the prospective tube has been produced. Its basic components were shown on Fig. 1. Their detailed construction has been completed as well. The main characteristics of the gyrotron under development are presented in Table 6. The calculations show that the operating modes could be excited without competition from the neighboring modes. It is expected that the novel gyrotron will be able to emit radiation at record levels of frequency and unprecedented high output power for such frequency range.

6 Conclusion

Design of a CW 1 THz gyrotron operating at second harmonic of the cyclotron frequency using a 20 T superconducting magnet has been described. The mode competition analysis is employed to investigate conditions for operation on several modes ($TE_{4,12}$, $TE_{8,10}$, $TE_{5,11}$, and $TE_{8,9}$) in the frequency range from 920 GHz to 1014 GHz. The output power up to 250 watt corresponding to the efficiency of 4.16 percent could be achieved by using electron beam with accelerating voltage 30 kV and current 200 mA. The important advantage of this gyrotron is that the single mode excitation at second harmonic, at extremely high frequency radiation could be maintained at the high current. It opens a possibility to realize a high power radiation source at 1 THz. The gyrotron is under construction at FIR Center, University of Fukui.

Acknowledgement This work was supported partially by Special Fund for Education and Research from the Ministry of Education, Culture, Sports, Science and Technology (MEXT) of Japan.

References

1. G. Dammertz, S. Alberti, A. Arnold, E. Borie, V. Ercmann, G. Gantenbein, E. Giguet, R. Heidinger, J. P. Hogge, S. Illy, W. Kasparek, K. Koppenburg, M. Kuntze, H. P. Laqua, G. LeCloarec, Y. LeGoff, W. Leonhardt, C. Lievin, R. Magne, G. Michel, G. Mueller, G. Neffe, B. Piosczyk, M. Schmid, K. Schwoerer, M. Thumm, and M. Q. Tran, "Development of a 140-GHz 1-MW continuous wave gyrotron for W7-X stellarator", IEEE Trans. Plasma Sci., **30**, 808–818 (2002)
2. M. Thumm, "MW gyrotron development for fusion plasma applications", Plasma Phys. Control. Fusion **45**, A143–A161 (2003)
3. V. E. Zapelov, G. G. Denisov, V. A. Flyagin, A. S. Fix, A. N. Kuftin, A. G. Litvak, M. V. Agapova, V. N. Ilyin, V. A. Khmara, V. E. Myasnikov, V. O. Nichiporenko, I. G. Popov, S. V. Usachev, V. V. Alikaev, and V. I. Ilyin, "Development of 170 GHz/1 MW Russian gyrotron for ITER", Fusion Eng. Des. **53**, 377–385 (2001)
4. K. Sakamoto, A. Kasugai, R. Minami, K. Takahashi, N. Kobayashi, T. Imai, "Development of high power 170 GHz gyrotron for ITER", in *Conf. Diggest of the 2004 Joint 29th Int. Conf. on Infrared and MM Waves and 12th Int. Conf. on Terahertz Electronics*, edited by M. Thumm and W. Wiesbeck (Univ. of Karlsruhe, Karlsruhe, 2004), pp 109–110.
5. T. Idehara, I. Ogawa, S. Mitsudo, M. Pareyaslavets, N. Nishida, and K. Yoshida, "Development of frequency tunable, medium power gyrotrons (Gyrotron FU Series) as submillimeter wave radiation sources", IEEE Trans. Plasma Sci. **27**, 340–354 (1999)
6. G. F. Brand, P. W. Fekete, K. Hong, K. J. Moore, and T. Idehara, "Operation of a tunable gyrotron at second harmonic of electron cyclotron frequency", Int. J. Electron. **68**, 1099–1111 (1990)
7. M. K. Hornstein, V. S. Bajaj, R. G. Griffin, and R. J. Temkin, "Continuous-wave operation of a 460-GHz second harmonic gyrotron oscillator", IEEE Trans. Plasma Sci. **34**, 524–533 (2006)
8. I. Ogawa, K. Yoshisue, H. Ibe, T. Idehara, and K. Kawahata, "Long-pulse operation of a submillimeter wave gyrotron and its application to plasma scattering measurement", Rev. Sci. Instrum. **65**, 1778–1789 (1994)
9. T. Tatsukawa, T. Maeda, H. Sasai, T. Idehara, M. Mekata, T. Saito, and T. Kanemaki, "ESR spectroscopy with a wide frequency range using a gyrotron as a radiation power source", Int. J. Infrared Millim. Waves **16**, 293–305 (1995)
10. S. Mitsudo, Aripin, T. Matsuda, T. Kanemaki, and T. Idehara, "High power, frequency tunable, submillimeter wave ESR device using a gyrotron as a radiation source", Int. J. Infrared Millim. Waves **21**, 661–676 (2000)
11. V. S. Bajaj, C. T. Farrar, M. K. Hornstein, I. Mastovsky, J. Vieregg, J. Bryant, B. Elena, K. E. Kreischer, R. J. Temkin, and R. G. Griffin, "Dynamic nuclear polarization at 9 T using a novel 250 GHz gyrotron microwave source", J. Magnetic Resonance **160**, 85–90 (2003)
12. T. Tatsukawa, A. Doi, M. Teranaka, H. Takashima, F. Goda, S. Watanabe, T. Idehara, T. Kanemaki, and T. Namba, "Microwave invasion through anti-reflecting layers of dielectrics at millimeter wave irradiation to living bodies", Int. J. Infrared Millim. Waves **26**, No. 4, 591–606 (2005)
13. T. Idehara, S. Mitsudo, S. Sabchevski, M. Glyavin, and I. Ogawa, "Gyrotron FU series-current status of development and applications", Vacuum **62**, 123–132 (2001)
14. I. Ogawa, T. Idehara, S. Maekawa, W. Kasparek, and G. F. Brand, "Conversion of gyrotron output into a gaussian beam using the far-field", Int. J. Infrared Millim. Waves **20**, No. 5, 801–821 (1999)
15. T. Idehara, H. Tsuchiya, O. Watanabe, La Agusu and S. Mitsudo, "The first experiment of a THz gyrotron with a pulse magnet", Int. J. Infrared and Millimeter Waves **27**, 319 (2006)
16. T. Saito, T. Idehara, S. Mitsudo, I. Ogawa, H. Hoshizuki, H. Murase, K. Sakai, V. E. Zapelov, O. V. Malygin, V. I. Khizhnjak, V. P. Karpov, and E. M. Tai, "Oscillation characteristics of CW 300 GHz gyrotron FU CW I," in *Conf. Digest of the 2006 Joint 31th Int. Conf. on Infrared and MM Waves and 14th Int. Conf. on terahertz electronics*, edited by S. C. Chen, W. Lu, J. Zhang, and W. B. Dou (Shanghai, China, 2006), p. 24.
17. La Agusu, H. Murase, T. Idehara, T. Saito, S. Mitsudo, D. Takahashi, and T. Fujiwara, "Design of a 400 GHz gyrotron for DNP-NMR spectroscopy," in *Conf. Digest of the 2006 Joint 31th Int. Conf. on Infrared and MM Waves and 14th Int. Conf. on Terahertz Electronics*, edited by S. C. Chen, W. Lu, J. Zhang, and W. B. Dou (Shanghai, China, 2006), p. 82.
18. T. Idehara, Y. Iwata, and I. "Ogawa, Observation of frequency-domain shift in a submillimeter wave gyrotron", Int. J. Infrared Millim. Waves **24**, 119–128 (2003)
19. T. Hori, T. Idehara, H. Sasagawa, A. Kimura, I. Ogawa, and S. Mitsudo, "Relationship among frequency, temperature of the cooling water and beam current in submillimeter wave gyrotron FU-IV", Rev. Sci. Instrum. **76**, 023502 (2005)

20. T. Idehara, I. Ogawa, S. Maeda, R. Pavlichenko, S. Mitsudo, D. Wagner, and M. Thumm, “Observation of mode patterns for high purity mode operation in the submillimeter wave gyrotron FU VA”, Int. J. Infrared Millim. Waves **23**, No. 7, 973–980 (2002)
21. A. N. Kuftin, V. K. Lygin, V. N. Manuilov, B. V. Raisky, E. A. Solujanova, and Sh. E. Tsimiring, “Theory of helical beams in gyrotrons”, Int. Jd. Infrared Millim. Waves **14**, 783–816 (1993)
22. N. A. Zavolsky, G. S. Nusinovich, and A. B. Pavelyev, “Stability of single mode oscillations and nonstationay processes in gyrotron with oversized low-quality resonators”, in *Gyrotrons*, Institute of Applied Physics, Academy of Sciences of the USSR, Gorky, Collection of scientific papers, edited by A. V. Gaponov-Grekhov (1989), pp. 84–112.